Liquid Crystals
Publication details, including instructions for authors and subscription information:
http://www.informaworld.com/smpp/title~content=t713926090

A new approach to lamellar phases (L_α) in water - non-ionic surfactant systems

C. Stubenrauch Corresponding author[a]; S. Burauer[a]; R. Strey[a]; C. Schmidt[b]
[a] Institut für Physikalische Chemie, Universität zu Köln, D-50939 Köln, Germany [b] Universität Paderborn, Fakultät für Naturwissenschaften, Department Chemie, D-33098 Paderborn, Germany

Online publication date: 19 May 2010

To cite this Article Stubenrauch Corresponding author, C. , Burauer, S. , Strey, R. and Schmidt, C.(2004) 'A new approach to lamellar phases (L_α) in water - non-ionic surfactant systems', Liquid Crystals, 31: 1, 39 — 53
To link to this Article: DOI: 10.1080/02678290310001628555
URL: http://dx.doi.org/10.1080/02678290310001628555

LIQUID CRYSTALS, VOL. 31, NO. 1, JANUARY 2004, 39–53

A new approach to lamellar phases (L_α) in water – non-ionic surfactant systems

C. STUBENRAUCH*, S. BURAUER†, R. STREY

Institut für Physikalische Chemie, Universität zu Köln, Luxemburger Str. 116, D-50939 Köln, Germany

†Technologiemarketing, Deutsches Zentrum für Luft- und Raumfahrt e.V. (DLR), Linder Höhe, D-51147 Köln

and C. SCHMIDT

Universität Paderborn, Fakultät für Naturwissenschaften, Department Chemie, Warburger Str. 100, D-33098 Paderborn, Germany

(*Received 23 May 2003; accepted 22 August 2003*)

We present new results on two unusual features concerning lamellar phases (L_α) in binary aqueous solutions of non-ionic surfactants. The first striking feature is the formation of highly dilute L_α phases down to 1 wt% of surfactant, which has been observed for a small number of non-ionic surfactants which are all of the alkyl polyglycol ether (C_iE_j) type. So far, in binary H_2O – C_iE_j systems either the absence or the presence of a dilute L_α phase has been reported. In the latter case, the dilute and the concentrated L_α phase are always connected continuously. However, for one particular silane surfactant, namely $(CH_3)_3Si(CH_2)_6(OCH_2$-$CH_2)_5OCH_3$, two disconnected L_α phases were observed. Systematic investigations of the phase behaviour of the binary H_2O – $C_{10}E_4$ system as well as of the pseudobinary H_2O – $C_{10}E_4/C_{10}E_5$ systems enabled us to conclude that: (a) the disconnected L_α phase is a general feature of non-ionic surfactants and (b) there are no structural differences between the connected and the disconnected L_α phases. We propose a mechanism for the disconnection of the L_α phase.

1. Introduction

In aqueous solutions of ionic surfactants, highly dilute lamellar phases which are stabilized by long range repulsive electrostatic forces have been observed [1–3]. In these papers phase diagrams of AOT [1] and DDAB [2, 3] are presented in which a dilute and a concentrated lamellar phase coexist. In the case of DDAB, Zemb *et al.* [3] showed that the coexistence vanished with increasing temperature. The authors argue: 'Increasing the temperature does not modify the electrostatic or van der Waals effects. But now a third repulsive force between the bilayers comes into play: it could be either protrusion or undulation forces.' We will see later that it is exactly this force that is responsible for the occurrence of a dilute lamellar phase in water–non-ionic surfactant sytems in which electrostatic forces are absent. Only about 13 years ago the lamellar phase of the binary system water – $C_{12}E_5$ (pentaethyleneglycol dodecyl ether) was found to swell to approximately 99 wt% of water [4]. This was a surprise since $C_{12}E_5$ is a non-ionic surfactant, i.e. stabilizing electrostatic forces are lacking, and the formation of a structured phase at surfactant concentrations as low as 1 wt% was not expected. Irrespective of the nature of the surfactant, dilute lamellar phases in binary water – surfactant systems are a peculiarity, which is underlined by the fact that up to now their formation has only been observed for a small number of systems [1–8]. A schematic phase diagram of a binary water – C_iE_j system including the dilute lamellar phase (L_α) is shown in figure 1.

Three features of this phase diagram are of relevance with respect to the discussion of the L_α phase. The first one is the intersection of the L_α phase with the upper miscibility gap; this intersection leads to a complex phase behaviour at low surfactant concentrations including several three-phase lines and two-phase regions. Another peculiarity is the broad concentration and temperature range over which the L_α phase exists. In some systems it is possible to dilute the L_α phase down to such low surfactant concentrations that the

*Author for correspondence;
e-mail: stubenrauch@uni-koeln.de

Liquid Crystals ISSN 0267-8292 print/ISSN 1366-5855 online © 2004 Taylor & Francis Ltd
http://www.tandf.co.uk/journals
DOI: 10.1080/02678290310001628555

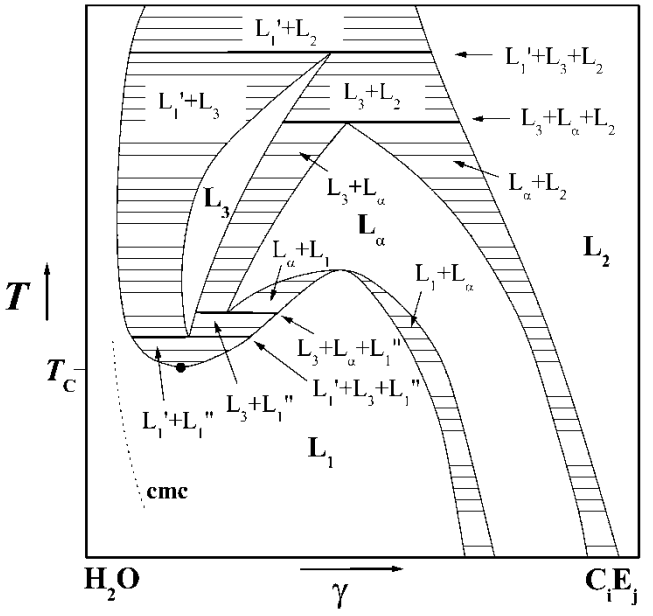

Figure 1. Schematic phase diagram of a binary system H_2O – C_iE_j (alkyl polyglycol ether) including the lamellar phase (L_α) and the isotropic sponge phase (L_3). L_1 and L_2 denote isotropic phases of normal and inverse micelles, respectively; T_c stands for the lower critical temperature and *cmc* for the critical micelle concentration. Two one-phase regions are separated by a two-phase region (hatched areas), whereas two two-phase regions are separated by a three-phase line (bold lines). Note that apart from the L_α phase a wide variety of different liquid crystalline phases exists. For the sake of simplicity they are not shown.

repeat distance of the lamellae is in the range of the wavelength of visible light. Hence, highly diluted L_α phases show an iridescence, the colour depending on the repeat distance and viewing angle. Last but not least, the presence of the sponge phase (L_3) in the vicinity of the dilute L_α phase may be mentioned. In an L_3 phase the bilayers form a three-dimensional random network. There exists visual evidence from freeze fracture electron microscopy [9] that this network develops from the lamellar phase by the formation of passages between the bilayers. The resulting structure is usually described as a sponge consisting of bilayers of zero mean curvature. The fact that the L_3 phase is only formed at low surfactant concentrations will be discussed later.

The influence of the molecular structure on the absence or presence of the dilute L_α phase can be demonstrated very well with the phase diagrams of binary water – C_iE_j systems. An important series are the $C_{12}E_j$ surfactants with $j=4$–6. Whereas for $j=4$ and 5 highly diluted lamellar phases are formed [5], which exist down to concentrations of 1 wt% ($C_{12}E_5$) or even less ($C_{12}E_4$), the phase diagram of $C_{12}E_6$ exhibits a lamellar phase only at concentrations higher than 60 wt% [10]. On the other hand, the decrease of the alkyl chain length from C_{12} to C_{10} can have the same effect as an increase of the hydrophilic headgroup, namely a suppression of the dilute region of the L_α phase. This tendency can be clearly seen when the phase behaviours of $C_{12}E_5$ and $C_{10}E_5$ are compared. For the former the lamellar phase extends from surfactant concentrations of about 90 wt% down to 1 wt% [4], whereas for the latter an L_α phase is only observed in a very small concentration range from 70–80 wt% [11]. Thus, starting from $C_{12}E_5$, a decrease of the alkyl chain length by two carbon atoms (from $C_{12}E_5$ to $C_{10}E_5$) as well as an increase of the headgroup length by one EO unit (from $C_{12}E_5$ to $C_{12}E_6$) dramatically changes the phase behaviour, i.e. completely suppresses the dilute L_α phase. In other words, both for a given alkyl chain a decrease of the headgroup length, and for a given headgroup an increase of the alkyl chain, lead to the formation of a dilute L_α phase.

The question arises as to what the phase diagrams of the 'intermediate' surfactants $C_{12}E_{5<j<6}$ and $C_{10<i<12}E_5$, respectively, would look like. It is true that surfactants with non-integral j do not exist, but surfactant mixtures can be investigated. In a systematic study of this kind, mixtures of two differently branched non-ionic surfactants were investigated [12]. The surfactant with the branched hydrophobic part (1) forms a broad lamellar phase, whereas in the phase diagram of the surfactant with the branched headgroup (2) a hexagonal phase and two cubic phases are observed. The addition of surfactant 2 to surfactant 1 leads to a continuous decrease of the lamellar phase region, which is accompanied by an increase of both the hexagonal and the cubic phases regions. Similarly, when adding $C_{12}E_6$ or $C_{10}E_5$ to $C_{12}E_5$ one expects a continuous reduction of the dilute L_α phase region until its formation is restricted to high concentrations, as is the case for the pure surfactants $C_{12}E_6$ and $C_{10}E_5$. However, the binary phase diagrams of a trisiloxane [7] and a trimethyl silane [8] surfactant, suggest a second possibility. Wagner and Strey [8] found that the surfactant $(CH_3)_3Si(CH_2)_6(OCH_2CH_2)_5OCH_3$ (which will be abbreviated as $(C_1)_3SiC_6E_5M$) stabilizes a lamellar phase down to concentrations of about 15 wt%. Surprisingly, the L_α phase formed at concentrations between 15 and 35 wt% is not connected with the L_α phase formed at higher concentrations, namely between 60 and 80 wt%. Similar features were observed for a trisiloxane surfactant, the hydrophilic part of which consists of 10 polyoxyethylene units [7]. In other words, two separate L_α phases are observed. The questions to be answered are the following. Is it possible to obtain

two disconnected L_α phases with C_iE_j surfactants? Are there any structural differences in the case of the two disconnected L_α phases? And last but not least, how can one follow experimentally the structural evolution along the concentration path?

To investigate the crossover from a system with one continuous lamellar phase extending to low concentrations to a system with a lamellar phase restricted to high concentrations upon changing the structure of the surfactant, we have chosen the $C_{10}E_j$ series, for which we expect similar changes in the phase diagram upon changing j as for the $C_{12}E_j$ series. First, for the $C_{10}E_j$ series a hydrophobicity similar to the corresponding trimethyl silane surfactants $(C_1)_3SiC_6E_jM$ is expected. Second, it is known from the previous work of Lang and Morgan [11] that the L_α phase of $C_{10}E_4$ intersects with the upper miscibility gap, a phenomenon which has already been observed for $C_{12}E_4$ and $C_{12}E_5$, the surfactants with known dilute L_α phases [4, 5, 10]. However, the exact extent of the L_α phase towards low surfactant concentrations is still unknown. Therefore, and in order to gain a deeper insight into the origin of the dilute L_α phase, we reinvestigated the phase diagram of $C_{10}E_4$, focusing on the dilute region. We found an L_α phase down to surfactant concentrations less than 10 wt%, which will be named the dilute L_α phase in the following discussion. Knowing that the formation of the L_α phase in the water – $C_{10}E_5$ system is restricted to concentrations above 70 wt% [11], mixtures of $C_{10}E_4$ and $C_{10}E_5$ were examined to determine the appearance of the phase diagrams of the 'intermediate' surfactants $C_{10}E_{4<j<5}$. The aim was to clarify whether the dilute L_α phase shrinks continuously only from the dilute side, remaining connected to the concentrated L_α region, or whether a separation of the dilute region from the concentrated one occurs. The structural evolution along a concentration path is monitored by ^{2}H NMR spectroscopy, from which the phase transitions and structural changes of lyotropic liquid crystals can be analysed very accurately [13–19]. First, with this technique it is easy to determine whether or not the lamellar phase coexists with an isotropic phase, which facilitates the interpretation of the phase diagrams. Second, the splitting of the ^{2}H NMR signal is a measure for the degree of order in the L_α phase, which helps in discussing the structural change from the dilute to the concentrated L_α phase.

2. Experimental

2.1. *Phase diagrams*

2.1.1. *Materials*

The non-ionic surfactants $C_{10}E_4$ and $C_{10}E_5$ with a purity >98% were purchased from Bachem Biochemica GmbH, Heidelberg, Germany. The purity of the surfactants can be judged by monitoring the critical temperature of the binary water – C_iE_j systems. The values known from the literature for the purified surfactants $C_{10}E_4$ and $C_{10}E_5$ are $T_c = 20.5°C$ at a mass fraction of $\gamma = 0.026$ [20] and $T_c = 40.25°C$ at $\gamma = 0.035$ [21], respectively. As the critical points for the purchased surfactants were determined to be only 0.5–0.7°C below the literature values, the surfactants were used without further purification. H_2O was ultrapure Millipore water, type Milli-Q RG. The D_2O needed for the ^{2}H NMR experiments was obtained from Cambridge Isotope Laboratories, Cambridge, MA, USA and used as purchased with an isotope purity >99%.

2.1.2. *Phase behaviour*

To determine the phase diagrams, desired amounts of water and surfactant were weighed in test-tubes equipped with Teflon coated stirring bars and sealed with polyethylene stoppers. The samples were thoroughly mixed and placed in a transparent water bath in which the temperature could be controlled to ± 0.02 K. The phase boundaries were determined by changing the water bath temperature in appropriate steps, thus reaching a precision of the phase transition temperatures of ± 0.05 K. The transition from a one-phase region to a two-phase region is kinetically hindered, which may cause incorrect boundary temperatures if only measured in that direction. Therefore phase boundaries were always confirmed by going from a two-phase to a one-phase region. From the equilibrated system the number and appearance of the phases were determined visually by inspection in scattered and transmitted light. Additionally, crossed polarizers were used to detect the birefringence at the $L_\alpha + L_3 \rightarrow L_3$ phase transition, since the L_α phase shows permanent birefringence, the L_3 phase just under shear. The composition of the binary and pseudobinary mixtures is characterized in terms of the total mass fraction of surfactant in the mixture

$$\gamma = \frac{m_{C_{10}E_4} + m_{C_{10}E_5}}{m_{H_2O} + m_{C_{10}E_4} + m_{C_{10}E_5}} \quad (1)$$

and the mass fraction of $C_{10}E_5$ in the surfactant mixture

$$\delta = \frac{m_{C_{10}E_5}}{m_{C_{10}E_4} + m_{C_{10}E_5}}. \quad (2)$$

2.2. *^{2}H NMR spectroscopy*

The ^{2}H NMR measurements were carried out with Bruker MSL 300 and Avance 500 spectrometers at a

deuterium resonance frequency of 46.07 and 76.78 MHz, respectively. For the measurements we used the spectrometer which was at our disposal. The samples were filled in 4 cm long glass tubes of 5 mm diameter, which were sealed with a Teflon plug and epoxy glue. The tubes were inserted into a home-built goniometer probe such that the tube axis was perpendicular to the static magnetic field. Spectra were measured with a quadrupole echo pulse sequence [22] and 16 scans were averaged before Fourier transformation. The temperature control of the probe was only ± 0.5 K, so care had to be taken to obtain the required phase. To keep the influence of the domain size on the quadrupole splittings to a minimum, measurements were performed on aligned lamellar samples. The sample was pre-equilibrated in the isotropic phase below or above the corresponding L_α phase (see phase diagrams). Slow heating or cooling from the isotropic to the anisotropic phase was sufficient to achieve a uniform alignment of the L_α phase by the magnetic field. For a perfectly aligned L_α phase the NMR spectrum is a well defined doublet, where $\Delta\nu$ is given by

$$\Delta\nu = 3/4\delta_Q(3\cos^2\theta - 1) \qquad (3)$$

where θ is the angle between the external magnetic field and the director (axis of symmetry) of the lamellar phase and $\delta_Q = e^2qQ/h$ is the quadrupole coupling constant averaged over the molecular motions of the water molecules (with e the elementary charge, h Planck's constant, eq the anisotropy of the averaged electric field gradient, and eQ the nuclear quadrupole moment) [22].

3. Results

3.1. *Phase diagrams*

Phase diagrams of the binary system H_2O – $C_{10}E_4$ and the pseudobinary system H_2O – $C_{10}E_4/C_{10}E_5$ are shown in figures 2 and 3. First, the phase behaviour of H_2O – $C_{10}E_4$ will be described in detail. Second, the influence of $C_{10}E_5$ on the binary system in general and on the extension of the lamellar phase in particular, will be shown. Last but not least, changes caused by the exchange of H_2O by D_2O will be presented. It has to be mentioned that according to the phase diagrams published by Lang and Morgan [11] a hexagonal phase is expected in both the binary and the pseudobinary systems. However, as the focus of the present study is on the lamellar phases, the hexagonal phases were not investigated in detail and were therefore not included.

3.1.1. *H_2O – $C_{10}E_4$*

The phase diagram of H_2O – $C_{10}E_4$ shown in figure 2 (*a*) was measured as a function of the temperature T and the surfactant mass fraction γ. To depict

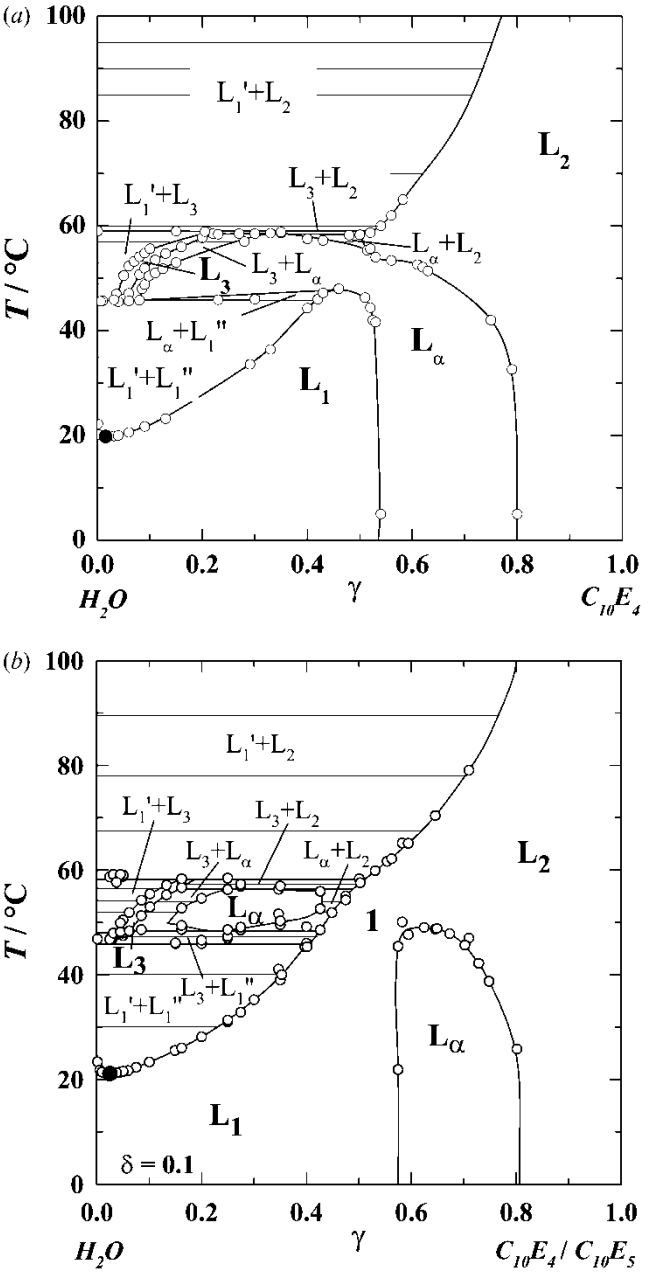

Figure 2. Phase diagrams of (*a*) the binary H_2O – $C_{10}E_4$ system and (*b*) the pseudobinary H_2O – $C_{10}E_4/C_{10}E_5$ system at $\delta = 0.10$. The indentation of the lamellar phase in the binary system at $T \approx 55$°C and $\gamma \approx 0.55$ is a first indication for the existence of two separate phases in the pseudobinary system. Hexagonal phases might be present but this possibility has not been examined. The notation is the same as in figure 1. In the case of the pseudobinary system, the labels L_1, 1, and L_2 are used to denote different regions of the single isotropic phase.

the real proportions of the different phase regions in the phase diagram, the concentration axis is drawn as a linear scale. As a result, the critical micelle concentration (*cmc*) cannot be represented in this

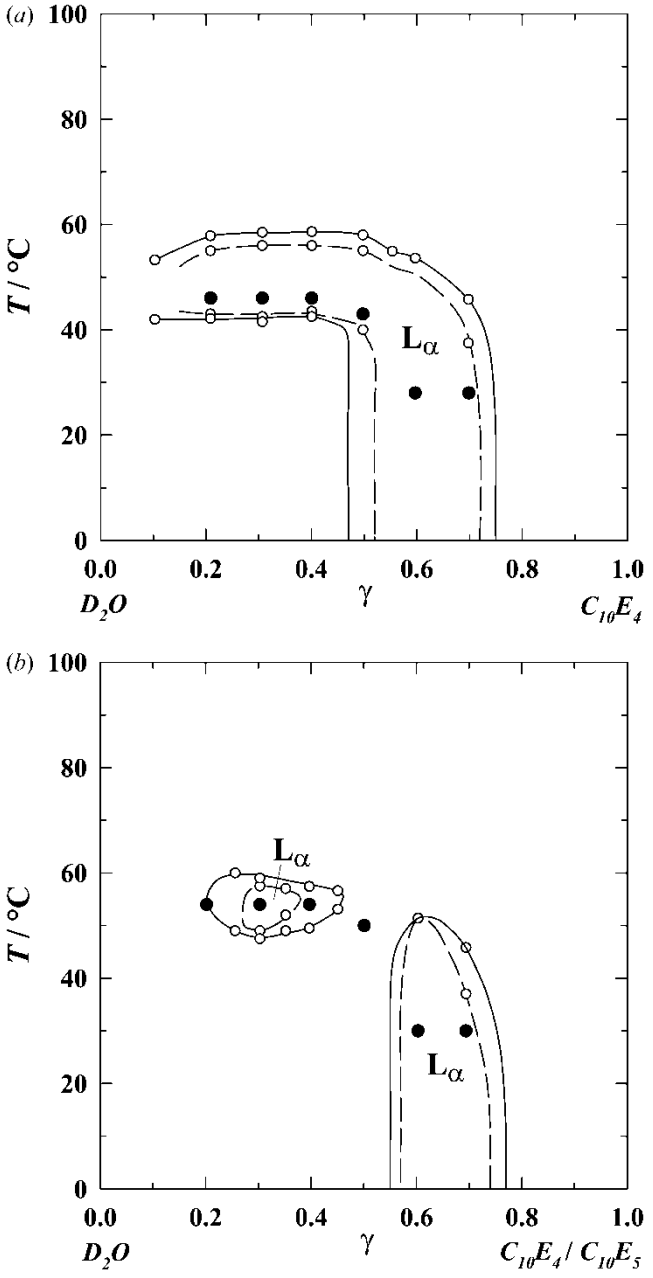

Figure 3. Extension of the L_α phase in the (*a*) binary D_2O – $C_{10}E_4$ system ($\delta=0$) and (*b*) the pseudobinary D_2O – $C_{10}E_4/C_{10}E_5$ system at $\delta=0.20$. The phase boundaries (lines) were estimated from the phase transitions (open symbols) determined by both visual inspection and ^2H NMR spectroscopy. The ^2H NMR spectra shown in figure 4 are recorded at the compositions and temperatures indicated in the phase diagrams (filled symbols).

diagram but is found experimentally to be $\gamma_{cmc}=3\times10^{-4}$ at $T=20°C$. The micellar L_1 phase extends up to the cloud point curve. The coordinates of the lower critical point (black dot), i.e. where the L_1 phase separates into a water-rich (L'_1) and a surfactant-rich (L''_1) phase, are $T_c=19.8°C$ and $\gamma_c=0.026$. The $L'_1+L''_1$ coexistence region extends to about 45°C. For higher temperatures, to about 59°C, the L_3 phase appears in the phase diagram as a narrow band, never wider than 4 K. It extends over a large concentration range from $\gamma=0.03$ to $\gamma=0.20$. The L_3 phase can easily be identified, for it is an optically isotropic fluid of low viscosity, which scatters light strongly and exhibits birefringence under shear. Over the same temperature range but shifted towards higher surfactant concentrations γ, the L_α phase can be observed. It extends far into the high concentration region of the phase diagram, where it reaches very low temperatures. In the high concentration region ($\gamma>0.50$) the L_α phase separates the micellar L_1 from its inverse counterpart, the L_2 phase. A point worth mentioning is the fact that at concentrations around $\gamma=0.55$ the phase boundary between the L_2 and the L_α phase is indented. Anticipating the observation that the pseudobinary H_2O – $C_{10}E_4/C_{10}E_5$ system forms two separate L_α phases, see figure 2 (*b*), one can interpret the 'dent' as an indication of the tendency to form an isotropic phase. As long as this tendency is restricted to a small concentration range two separate L_α phases can be observed.

3.1.2. H_2O – $C_{10}E_4/C_{10}E_5$

Having found that $C_{10}E_4$ forms an L_α phase from 80 wt% down to 8 wt%, while the L_α phase of $C_{10}E_5$ is restricted to 70–82 wt%, we decided to investigate mixtures of these two surfactants to monitor the suppression of the L_α phase at low surfactant concentrations. The main objective of the present work was to clarify whether the L_α phase shrinks continuously, or there is first a separation of the lamellar region before the L_α phase in the dilute region eventually vanishes. For that purpose, a $C_{10}E_4/C_{10}E_5$ mixture with $\delta=0.10$ (mass fraction of $C_{10}E_5$ in the surfactant mixture) was chosen. The choice of $\delta=0.10$ is explained in Appendix 1. The corresponding T–γ phase diagram of this mixture is shown in figure 2 (*b*). Comparing figures 2 (*a*) and 2 (*b*), one clearly sees the influence of $C_{10}E_5$ on the phase behaviour of the H_2O – $C_{10}E_4$ system. While the isotropic phases are not strongly affected, a significant change of the L_α region is observed. Instead of one broad lamellar region, two disconnected regions appear, one in the concentration range $0.14\leqslant\gamma\leqslant0.43$, the other in the range $0.58\leqslant\gamma\leqslant0.80$. The corresponding temperatures are 48.6–56.4°C and $T<49°C$, respectively. Thus an increase of δ from 0 to 0.10 induces a phase transition from an L_α to an isotropic phase between $\gamma=0.43$ and $\gamma=0.58$. The nature of the isotropic phase remains to be clarified. We will return to this point in the discussion. The phase diagram shown in figure 2 (*b*)

is the first experimental evidence of disconnected L_α phases in a C_iE_j system. Obviously, disconnected lamellar phases are not a characteristic feature of the surfactant $(C_1)_3SiC_6E_5M$ investigated by Wagner and Strey [8] but rather a general phenomenon which will be discussed later.

3.1.3. *Influence of D_2O*

Comparing figures 3 (*a*) and 2 (*a*), one clearly sees that the exchange of H_2O by D_2O does not result in the commonly observed decrease of the boundaries of isotropic phases by 2–3 K [19, 23]. On the contrary, the upper phase boundary of the L_α phase is shifted slightly towards higher temperatures by 1–2 K. This shift decreases with increasing surfactant concentration until at $\gamma = 0.70$ the phase transition from L_2 to $L_\alpha + L_2$ takes place at the same temperature for both the H_2O – $C_{10}E_4$ and the D_2O – $C_{10}E_4$ systems. In addition to the shift of the upper phase boundary towards higher temperatures, a decrease of the lower phase boundary by 3–4 K can be seen for $\gamma < 0.50$. Therefore, at concentrations below 0.50 the temperature range in which the lamellar phase is formed increases by approximately 5 K, whereas its range is unaffected at higher concentrations. However, it is not only on the temperature scale that the L_α phase becomes more stable but also on the concentration scale. In the protonated system the low concentration limit is reached at $\gamma = 0.08$, figure 2 (*a*).

With D_2O, the range of the L_α phase towards low surfactant concentrations was not measured. However, the phase diagram shown in figure 3 (*a*) suggests that a formation of the L_α phase at concentrations below $\gamma = 0.08$ is very likely. A higher swelling with D_2O would be in agreement with observations made for the binary H_2O – $C_{12}E_5$ and D_2O – $C_{12}E_5$ systems [4]. Note that for a quantitative comparison, volume instead of mass fractions have to be considered. To summarize, the formation of the dilute L_α phase is favored in the presence of D_2O, whereas the phase behaviour at high surfactant concentrations is not influenced by the exchange of H_2O by D_2O. Remembering the evolution of the lamellar phase in the C_iE_j series, one realizes that the surfactant behaves as if it were more hydrophobic in the presence of D_2O than in the presence of H_2O. So far, only a qualitative explanation for this observation can be given. It is known that the O–D bond is stronger than the O–H bond so that the hydration of the hydrophilic headgroup might be expected to be stronger in the presence of D_2O. A stronger hydration leads to a shift of the miscibility gap towards higher temperatures. However, the opposite is observed. Speculative as it may be, we believe that a stronger hydrophobic effect in D_2O is the explanation for the experimental observations. In other words, the interactions between the alkyl chain and D_2O are less favourable than those between the alkyl chain and H_2O. Thus, a possibly stronger hydration of the hydrophilic part in D_2O is outweighed by the dehydration of the hydrophobic part, which leads to a surfactant with a hydrophobicity that is somewhat higher than in H_2O.

Not surprisingly, the increase in the stability of the L_α phase also influences the phase behaviour of the pseudo-binary D_2O – $C_{10}E_4/C_{10}E_5$ system. The effect is well demonstrated for the mixture with $\delta = 0.10$. While two separate lamellar regions are observed in the protonated system, figure 2 (*b*), in the deuterated system the L_α phase is still connected (see Appendix 2). As the aim of the present paper was to study the disconnected L_α phase, the amount of $C_{10}E_5$ in the $C_{10}E_4/C_{10}E_5$ mixture was further increased to induce the separation. Indeed, as can be seen in figure 3 (*b*), two separate phases were observed for $\delta = 0.20$ and thus this mixture was chosen to perform the NMR measurements.

3.2. *^2H NMR spectroscopy*

To monitor phase transitions and structural changes in the L_α phase, ^2H NMR spectroscopy was chosen. The focus will be on a series of spectra measured along a concentration path through the lamellar region. A splitting of the spectra indicates anisotropic mesophases, whereas a single peak results for isotropic phases. The splitting does not serve only as experimental evidence for the presence of an anisotropic phase, i.e. an L_α phase for the systems at hand, but also as a measure for the degree of order in this phase. To be more precise, in D_2O – surfactant systems a splitting indicates that the averaged motion of the water molecules is anisotropic. As the exchange between hydration water and water that is free to move is fast on the NMR timescale, an averaged motion is detected. Thus, the splitting is a measure for the amount of hydration water bound to an anisotropic phase. In the following, the spectra and the corresponding splittings will be presented for both the D_2O – $C_{10}E_4$ and the D_2O – $C_{10}E_4/C_{10}E_5$ systems. Concentration- and temperature-dependent measurements were performed to gain a deeper insight into the phenomenon of dilute L_α phases.

3.2.1. *Spectra*

In figure 4 (*a*) spectra of the D_2O – $C_{10}E_4$ system are shown as a function of the surfactant concentration γ. In a concentration range $0.20 \leqslant \gamma \leqslant 0.70$ spectra were recorded in steps of 0.10. For each concentration,

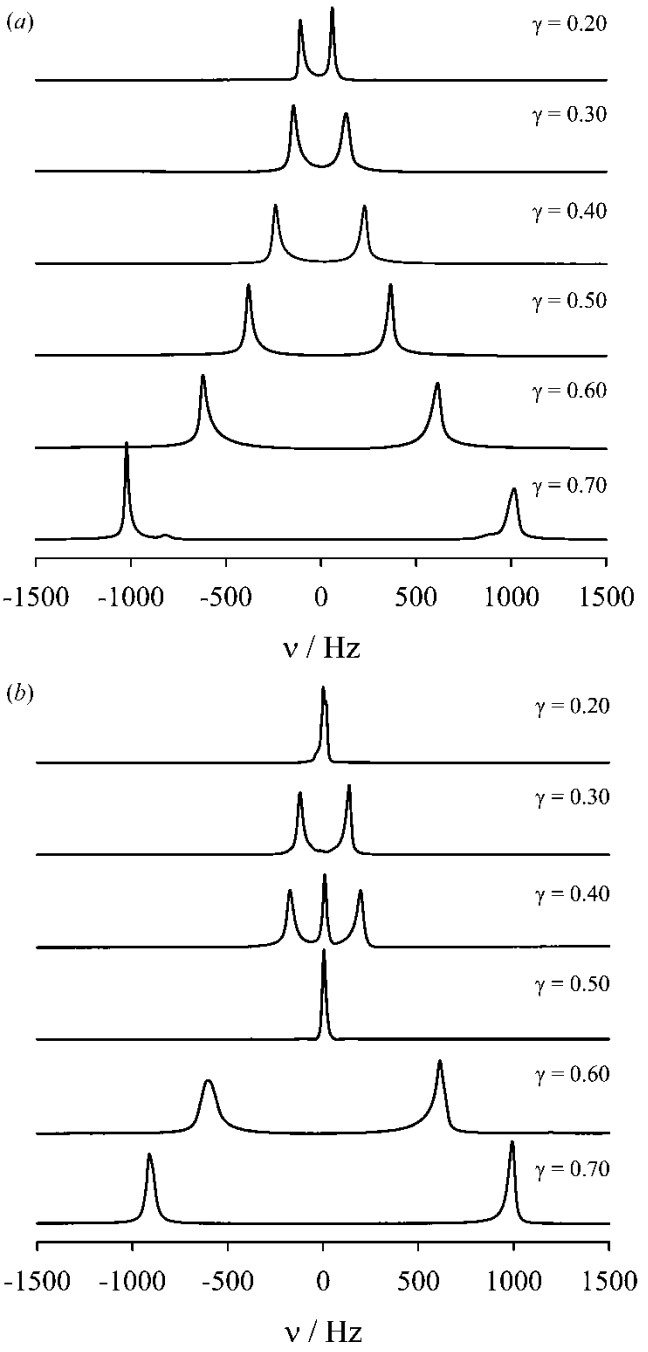

Figure 4. (*a*) ^{2}H NMR spectra of the D_2O – $C_{10}E_4$ system along a concentration path through the lamellar region. The temperatures at which the spectra were recorded are $T=46°C$ for $\gamma=0.2$, 0.3 and 0.4, $T=43°C$ for $\gamma=0.5$ and $T=28°C$ for $\gamma=0.6$ and 0.7 (see text for explanation). The samples are shown in figure 3 (*a*). (*b*) ^{2}H NMR spectra of the D_2O – $C_{10}E_4/C_{10}E_5$ system along a concentration path through the lamellar region. The temperatures at which the spectra were recorded are $T=54°C$ for $\gamma=0.2$, 0.3 and 0.4, $T=50°C$ for $\gamma=0.5$ and $T=30°C$ for $\gamma=0.6$ and 0.7 (see text for explanation). The samples are shown in figure 3 (*b*).

temperature-dependent measurements were performed from which the spectra with the broadest splitting are shown in figure 4 (*a*). The compositions and temperatures of the samples are shown in figure 3 (*a*). The evolution of the lamellar phase is clearly seen: a single anisotropic phase is formed, the splitting of which increases continuously with the surfactant concentration. From the temperature scans (spectra not shown) the phase boundaries of the L_α phase, i.e. $L_\alpha \rightarrow L_\alpha +$ isotropic$\rightarrow$isotropic, were determined; the results are shown in figure 3 (*a*). In contrast to the spectra of the binary system, those of the pseudobinary D_2O – $C_{10}E_4/C_{10}E_5$ system, which are shown in figure 4 (*b*), clearly demonstrate two separate lamellar regions. The lamellar phase observed at low concentrations is restricted to concentrations of about $0.25<\gamma<0.40$ and surrounded by a broad two-phase region (see spectrum for $\gamma=0.20$ and 0.40).† At concentrations above 0.50 a second L_α phase was found. In contrast to the L_α phase observed at low γ, the one at high γ is stable over a broad temperature range. The phase between the two lamellar phases is found to be isotropic (see spectrum for $\gamma=0.50$). With this sequence, phase transitions and coexistence regions could be identified.

It is important to stress how this information about the two-phase regions complements the results of the visual inspection. From the latter we know that an L_α phase is formed in a concentration range $0.20<\gamma<0.50$ at temperatures between 50 and 60°C. The NMR measurements led to the result that it is not the extension of a single anisotropic phase but mainly that of the adjacent two-phase region which is seen in the macroscopic test tubes. The resulting phase boundaries are shown in figure 3 (*b*).

3.2.2. *Splitting*

With respect to the evaluation of the quadrupole splittings $\Delta\nu$ we will focus on the D_2O – $C_{10}E_4$ system. For the pseudo-binary D_2O – $C_{10}E_4/C_{10}E_5$ system only a few $\Delta\nu$ values will be shown as most of the spectra were recorded in two-phase regions.‡ The splittings of

†For the samples with $\gamma=0.25$, 0.40 and 0.45 the coexistence of two phases (isotropic + L_α) was observed over the whole temperature range, whereas for $\gamma=0.30$ and 0.35 a single lamellar phase surrounded by the corresponding two-phase region was detected.

‡The two-phase regions we are dealing with are those in which the L_α phase coexists with an isotropic phase. The splitting that is observed corresponds to the coexisting L_α phase. As neither the composition nor the amount of the coexisting L_α phase are known precisely, a comparison with the splitting of the one-phase region is unreasonable. On the contrary, it is from the $\Delta\nu(\gamma)$-curve of the one-phase region that the composition of the coexisting L_α phase can be deduced.

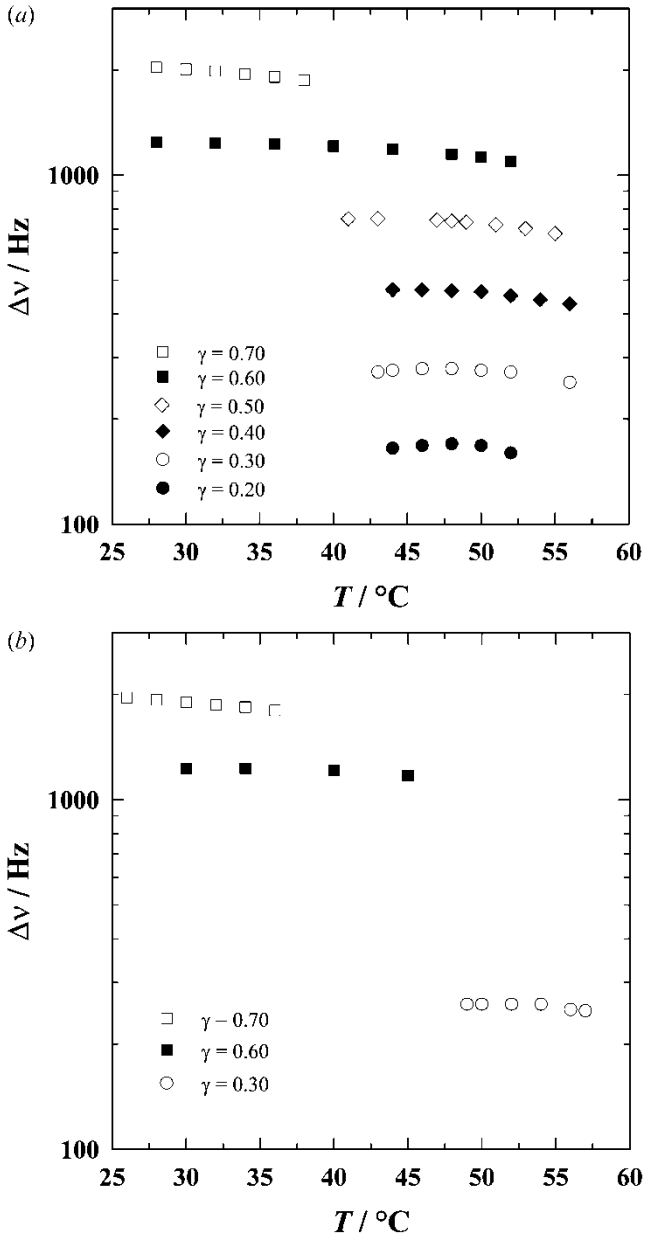

Figure 5. (*a*) Quadrupole splittings $\Delta\nu$ of the D_2O – $C_{10}E_4$ system for six concentrations γ as a function of the temperature T. (*b*) Quadrupole splittings $\Delta\nu$ of the D_2O – $C_{10}E_4/C_{10}E_5$ system for three concentrations as a function of the temperature T.

the D_2O – $C_{10}E_4$ system are shown in figure 5 for six different concentrations γ as a function of temperature T. The $\Delta\nu$ values are plotted on a log-scale to present all data in one figure.

It is clearly seen that $\Delta\nu$ decreases with decreasing surfactant and thus decreasing lamellae concentration. This is because $\Delta\nu$ is a measure of the fraction of water bound to the lamellae-forming surfactants. However, the amount of bound water does not only depend on the surfactant concentration but also on the temperature. Knowing that the hydration degree of C_iE_j surfactants decreases with increasing temperature, one expects that an increase in temperature is accompanied by a decrease of the splitting. Indeed, a continuous decrease of $\Delta\nu$ with increasing temperature is found for $\gamma = 0.70$. However, for $\gamma = 0.60$, 0.50 and 0.40 a plateau, and for $\gamma = 0.30$ and 0.20 even a maximum, is observed in the $\Delta\nu(T)$-curves. The temperature dependence of $\Delta\nu$ reflects the change of the overall ordering of the phase. In other words, deviations from extended smooth lamellae of zero curvature cause a decrease of the splitting [17]. Thus, the maximum in the $\Delta\nu(T)$-curves represents the L_α phase of highest order. On decreasing or increasing the temperature, defects occur causing the decrease of the splitting. As can be seen in figure 5 (*b*), the same trend, namely a levelling off of the $\Delta\nu(T)$-curve with decreasing surfactant concentration, is found for the pseudobinary system. While for $\gamma = 0.70$ an increase of the temperature leads to a continuous decrease of $\Delta\nu$, the splittings of the samples with $\gamma = 0.60$ and 0.30 reach a plateau at low temperatures. The $\Delta\nu$ values corresponding to the maxima and plateau values are shown in figure 6 as a function of γ.

For the interpretation of the $\Delta\nu_{max}$ values, two issues have to be considered. First, for $\gamma = 0.70$ the splittings are expected to increase further with decreasing

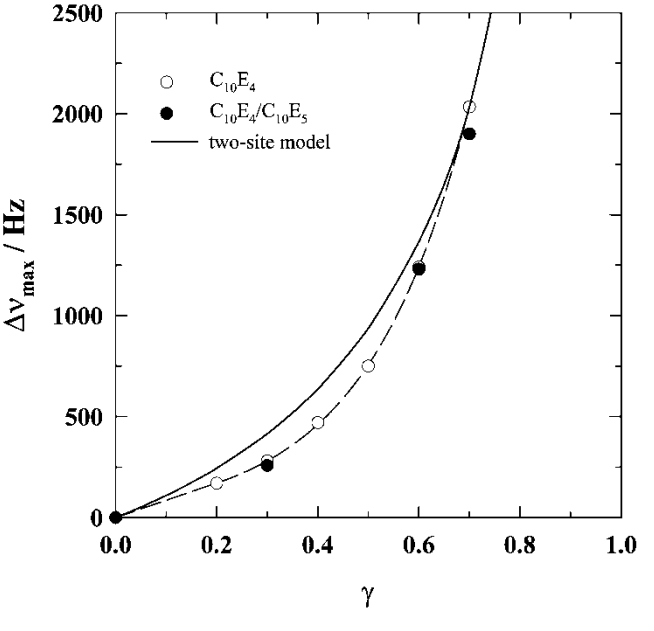

Figure 6. Maximum quadrupole splittings $\Delta\nu_{max}$ of the D_2O – $C_{10}E_4$ and D_2O – $C_{10}E_4/C_{10}E_5$ systems as a function of the surfactant concentration γ. The corresponding spectra are shown in figure 4. The theoretical $\Delta\nu(\gamma)$-curve represents the two-site model and was calculated with equation (5).

temperature. However, an extrapolation of the data shown in figure 5 towards lower temperatures leads to a maximum increase of the $\Delta\nu$ values by around 100 Hz, an increase which is not relevant for the $\Delta\nu_{max}(\gamma)$-curve shown in figure 6. Second, the $\Delta\nu_{max}$ values shown in figure 6 correspond to different temperatures. However, as the effect of temperature on the splitting is very low compared with the effect of concentration, the maximum splittings can be compared without a correction for the temperature effect.

The dependence of the quadrupole splitting $\Delta\nu$ on the surfactant mass fraction γ can be described using a simple two-site model [24]. In this model a distinction is made between bound water and water that is free to move. The experimentally determined $\Delta\nu$ value is a measure of the amount of water molecules bound to the anisotropic phase, i.e. $\Delta\nu = x_b\,\Delta\nu_b$, where x_b is the mole fraction of bound water and $\Delta\nu_b$ the quadrupole splitting for bound water molecules. It should be noted that the exchange between bound and free water is so fast that no isotropic peak but a reduced splitting is seen for $x_b < 1$. The mole fraction of bound water x_b is given by [24]

$$x_b = n_b \frac{M_w\gamma}{M_w\gamma + M_s(1-\gamma)} \qquad (4)$$

where n_b is the number of bound water molecules per surfactant headgroup (hydration degree) and M_s and M_w are the molecular masses of surfactant and water (D_2O here), respectively. According to equation (4) the following relationship between $\Delta\nu$ and the surfactant mass fraction γ is expected:

$$\Delta\nu = n_b \frac{M_w\gamma}{M_w\gamma + M_s(1-\gamma)} \Delta\nu_b. \qquad (5)$$

As neither n_b nor $\Delta\nu_b$ were known, we proceeded as follows. Kilpatrick *et al.* investigated the quadrupole splittings of a lamellar phase at concentrations above 60 wt% ($\gamma > 0.6$) [24]. They found that the experimental $\Delta\nu$ values conform well to equation (5) for $n_b\Delta\nu_b$ equal to 9 500 Hz. Thus, we took the splitting of the highest concentration investigated here, i.e. $\Delta\nu = 2\,034$ Hz and $\gamma = 0.7$, to calculate the factor $n_b\Delta\nu_b$. From equation (5) a value of 16 600 Hz was obtained; the resulting $\Delta\nu(\gamma)$-curve is seen in figure 6. In contrast to the observations made by Kilpatrick *et al.* [24], the experimentally observed splittings deviate from the theoretical model. We will return to this deviation in the discussion.

4. Discussion

The two unusual features of the L_α phases observed in aqueous solutions of non-ionic surfactants, namely the formation of a highly diluted L_α phase and the disconnection of the lamellar region, will be dealt with in the following discussion. First, the results presented here will be compared with results published to date. Second, different mechanisms stabilizing the L_α phase and the process leading to the disconnection will be discussed.

4.1. *The phenomenon of connected and disconnected L_α phases*

4.1.1. *Connected L_α phases*

The reports of highly diluted L_α phases in binary water – non-ionic surfactant systems are restricted to a small number of surfactants, all of which are of the alkyl polyglycol ether type. The 'record' is the formation of L_α phases down to 1 wt% surfactant as observed for $C_{12}E_5$ and $C_{12}E_4$ [4, 5]. In the $C_{10}E_j$ series investigated here, a dilute L_α phase is observed for $j = 3$ [25, 26] and $j = 4$. Although the published phase diagram of $C_{10}E_3$ can only be considered as being preliminary in nature because many details are lacking, it is obvious that the dilute lamellar phase extends down to lower surfactant concentrations than in the corresponding binary water – $C_{10}E_4$ system. For the $C_{10}E_5$ homologue an L_α phase is only observed in the very small concentration range 70–80 wt% [11].

Apart from the surfactants $C_{12}E_5$, $C_{12}E_4$, $C_{10}E_4$ and $C_{10}E_3$, highly dilute L_α phases were observed for three surfactants whose hydrophobic parts are branched [6, 7]. It is primarily the branched surfactant $C_4C_iGE_8M$ series which is of interest with respect to the formation of dilute L_α phases [6]. These surfactants consist of a triglyceryl unit (G) which connects two different alkyl chains (C_4 and C_i) with the hydrophilic headgroup E_8M (E_8, terminated by OCH_3). The L_α phase is found to extend from 8 to 80 wt% in the binary H_2O – $C_4C_{10}GE_8M$ system and from 2 to 83 wt% in the H_2O – $C_4C_{12}GE_8M$ system. In addition, the temperature range over which the L_α phase exists is increased in the latter system. It is a well known and therefore hardly surprising phenomenon that a shortening of the alkyl chain causes a destabilization of the L_α phase region. However, for these particular surfactants the destabilization is accompanied by an indentation. Similar to the observations made for H_2O – $C_{10}E_4$, the phase boundary of the H_2O – $C_4C_{10}GE_8M$ system is indented around 50 wt%, a phenomenon not seen for $C_4C_{12}GE_8M$. Interpreting this indentation as a first step towards a disconnection of the L_α phase, one expects the formation of two separate L_α phases with a further decrease of the number of C-atoms in the C_i chain. The fact that the dent in the phase boundary occurs around 50 wt% for both H_2O – $C_4C_{10}GE_8M$ and H_2O – $C_{10}E_4$ will be explained later.

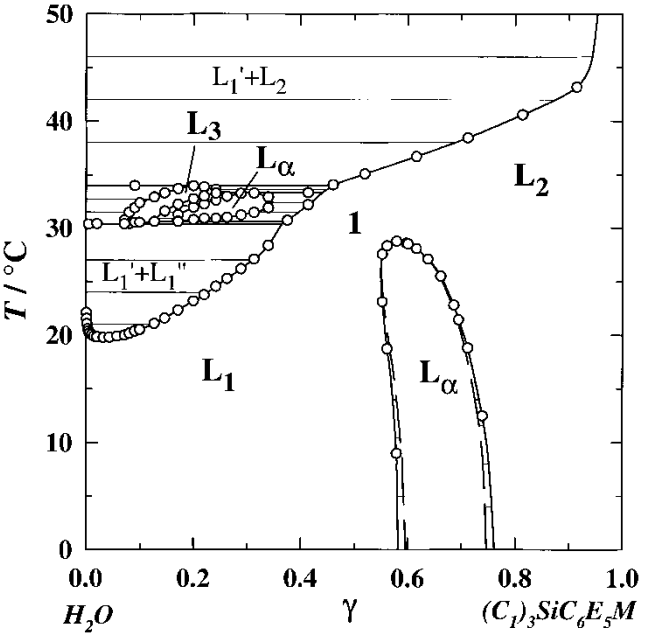

Figure 7. Phase diagram of the binary H_2O – $(CH_3)_3Si(CH_2)_6(OCH_2CH_2)_5OCH_3$ system [8]. Note that the temperature scale ranges only from 0 to 50°C, whereas in figures 2 and 3 it is from 0 to 100°C. The notation is the same as in figure 1.

4.1.2. *Disconnected L_α phases*

We have seen that the number of surfactants known to stabilize a dilute L_α phase is very small. Presumably, a precisely balanced molecular structure is needed for its formation (we will return to this point in §4.2). The requirements for the molecular design seem to be even 'harder' for the formation of two separate L_α phases. The trimethyl silane surfactant $(C_1)_3SiC_6E_5M$, for example, seems to fulfill these requirements. Comparing figure 7 with figure 2 (*b*), one clearly sees the similarities between the two phase diagrams. The only significant difference concerns the temperatures at which the phase transitions occur. With respect to temperature, the extensions of the phases observed for the trimethyl silane surfactant are about half of those observed for the $C_{10}E_4/C_{10}E_5$ mixture. Nevertheless, the phase diagrams are surprisingly similar, so that it is justifiable to say that the phase behaviour of $(C_1)_3SiC_6E_5M$ parallels that of the $C_{10}E_4/C_{10}E_5$ mixture with $\delta = 0.1$, which corresponds to the hypothetical surfactant $C_{10}E_{4.1}$. Going one step further, one can argue that the phase behaviour of $C_{10}E_4$ is expected to be the same as that of the hypothetical surfactant $(C_1)_3SiC_6E_{4.9}M$. Thus, the substitution of 10 wt% $(C_1)_3SiC_6E_5M$ by $(C_1)_3SiC_6E_4M$ is expected to lead to a connection of the two separate lamellar regions.

To conclude, one can say that the phenomenon of disconnected L_α phases is a general feature of non-ionic surfactants. It is simply by chance that molecular structures which are easy to synthesize do not fulfill the requirements for the formation of a disconnected L_α phase. Thus, in order to tune the phase behaviour precisely, a way has to be found by which the structure can be changed in very small steps. We have shown that the crossover from a system with one continuous L_α phase extending to low concentration, to a system with an L_α phase restricted to high concentrations, can be investigated by mixing the corresponding surfactants. As mentioned already in the introduction, the approach of using mixed surfactants to tune the phase behaviour has also been used successfully in a systematic study of two differently branched non-ionic surfactants [12].

Thus, the method of choice for detailed investigation of phase transitions as a function of the molecular structure is the use of surfactant mixtures. From the results presented here, it can be deduced that the crossover between connected and disconnected L_α phases can be induced by mixing appropriate surfactants, for example $C_{10}E_4$ and $C_{10}E_5$, $C_{12}E_5$ and $C_{12}E_6$, $C_4C_{10}GE_8M$ and $C_4C_8GE_8M$ and, last but not least, the trimethylsilane surfactants $(C_1)_3SiC_6E_4M$ and $(C_1)_3SiC_6E_5M$.

4.2. *The process leading to the disconnection of the L_α region*

4.2.1. *Structural evolution in the L_α region*

First we would like to address the question whether or not there are structural differences between the connected and disconnected L_α phases. An answer to this question might be provided by the concentration-dependent splittings obtained from the ^2H NMR measurements. It can be seen in figure 6 that the splitting, i.e. the order of the L_α phase, increases continuously with increasing surfactant concentration. Furthermore, for a given concentration, the splittings of the pseudo-binary system are the same as those of the binary system. This clearly demonstrates that it is only the extension but not the structure of the L_α phase that is changed by substituting $C_{10}E_4$ by $C_{10}E_5$. These results are not in agreement with the measurements made by Kratzat *et al.* [18]. In their work an abrupt increase of the quadrupole splitting was found at concentrations between 50 and 60 wt% and interpreted as a change of the lamellar structure. It should be noted that the results presented in [18] are not consistent. Specifically, while a continuous decrease of the interlamellar distance is observed by X-ray diffraction, two different lamellar structures are deduced from the NMR results.

With respect to the system at hand, it is seen in

figure 6 that the theoretical two-site model does not describe the measured splittings over the whole concentration range. Assuming that the deviation is not due to a change in the degree of hydration, there must be a different origin of this phenomenon.§ The presence of undulations, which are not considered in the two-site model, is consistent with the observation made in figure 6. Owing to thermally induced undulations, the bilayers are only flat on average. Thus, the average order of the hydration water is reduced, resulting in a reduced splitting. In other words, the difference between the experimental and theoretical results is a measure of the degree of undulations. In addition, passages between the lamellae would also be consistent with the reduced splittings, as D_2O molecules can exchange between the interconnected lamellae and thus reduce the observed anisotropy. A complex interplay between these two competing effects is assumed, a separation of which is not possible. To summarize the results of the NMR measurements, the lamellar structure changes continuously along the chosen concentration path. The deviation from the theoretical two-site model is a measure of defects in the lamellar structure owing to undulations and/or passages between the lamellae (so-called interlamellar attachments [27]). However, an indication of the indentation or the disconnection is not given.

4.2.2. *Stabilization of L_α phases*

As the structural evolution does not indicate the disconnection we have to look in more detail at the mechanisms which stabilize—or destabilize—the L_α phase. First it has to be understood what requirements a surfactant has to fulfill in order to stabilize an L_α phase in general and a dilute L_α phase in particular. To answer this question two factors must be considered, namely the structure of the single molecule and the rigidity of the surfactant monolayer, which are interrelated. In general, an L_α phase is formed when the ratio of the hydrophilic to the hydrophobic area is balanced, i.e. $a_{head}/a_{chain} \approx 1$. For a given surfactant, the area of the hydrophobic chain is constant, whereas the area of the headgroup depends on the degree of hydration. Dehydration can be forced by both an increase in the temperature and an increase in the surfactant concentration (less water is available), which explains why the temperatures at which the dilute L_α phase is formed are much higher than those of the concentrated L_α phase. However, it is not only the a_{head}/a_{chain} ratio but also the rigidity of the surfactant layer which plays a role. It is only above a certain rigidity that L_α phases can be stabilized, which becomes obvious when one compares the phase diagrams of $C_{12}E_4$ [5], $C_{10}E_4$ (figure 2 (*a*)), and C_8E_4 [10]. Whereas $C_{12}E_4$ and $C_{10}E_4$ form a broad L_α phase, for C_8E_4 an L_α phase exists at neither low nor high concentrations. As the ratio a_{head}/a_{chain} does not change significantly, these observations can only be explained by a decrease in the rigidity of the monolayers. The rigidity may be interpreted as a measure of the intermolecular forces between the molecules forming the monolayer (cohesive attraction). Thus, the stronger these forces, the more rigid the monolayer. Indeed, it was shown with SANS measurements in microemulsions that the corresponding rigidity constants κ of the surfactant layers decrease significantly from $C_{12}E_4$ to C_8E_4 [28]. The values are given in the table.

Furthermore, it can be concluded from the values given in the table that for the formation of a dilute L_α phase at high temperatures (which are needed for the dehydration) a higher rigidity is needed than for the formation of a concentrated L_α phase. This is due to the fact that the undulations are stronger the higher the temperatures, so that a membrane of high rigidity is required to sustain these fluctuations. (Note that $C_{12}E_6$ does not form a dilute L_α phase although its rigidity constant κ is higher than that of $C_{10}E_4$. This is because for the hydrophilic $C_{12}E_6$ a dilute L_α phase is expected to form at much higher temperatures than the corresponding L_α phase of $C_{10}E_4$. Obviously an even higher κ is required to stabilize a dilute L_α phase at these temperatures.)

Table. Rigidity constants κ obtained from a SANS study of C_iE_j surfactants at the water – *n*-octane interface and the temperature T at which the respective measurements have been performed [28]. Phase diagram studies of the binary water – C_iE_j systems revealed that in addition to the L_α phase formed at high surfactant concentrations a dilute L_α phase is observed for $C_{10}E_4$, $C_{12}E_4$, and $C_{12}E_5$.

Surfactant	κ/kT	T/°C	dilute L_α?
C_8E_4	0.51	39.5	no[a] [10]
$C_{10}E_4$	0.73	22.7	yes[b]
$C_{10}E_5$	0.65	42.2	no [11]
$C_{12}E_4$	1.06	11.0	yes [5]
$C_{12}E_5$	0.92	30.6	yes [5]
$C_{12}E_6$	0.81	46.8	no [10]

[a]Lamellar phase exists at neither low nor high concentrations.
[b]Figure 2 (*a*) in this paper.

§The hydration degree n_b was assumed to be constant to calculate the prefactor $n_b\Delta\nu_b$ in equation (5). This is justified by the fact that we evaluated the $\Delta\nu_{max}$ values, i.e. the splittings at which n_b is maximum for the given concentration γ. At this particular hydration degree the order of the lamellar phase reaches its maximum, which corresponds to a zero curvature. As the curvature in the binary systems can only be adjusted via the hydration degree of the hydrophilic head, an equal curvature is tantamount to an equal hydration degree.

Knowing that a surfactant of balanced molecular structure and a significant rigidity of the surfactant layer are required to stabilize an L_α phase, we can return to the question why the L_α phase is disconnected at intermediate surfactant concentrations. The basic forces between two parallel non-charged lamellae are long range attractive van der Waals and short range repulsive hydration forces. In addition, thermally induced layer undulations are proposed [29], the driving force of which is the increase of configurational entropy. As long as the interlamellar distance d is in the range of (or even lower than) the membrane thickness ε, the Helfrich interaction is outweighed by the van der Waals attraction. However, for $d > \varepsilon$ the undulation force dominates. Thus, at low concentrations, i.e. high interlamellar distances d, repulsive undulation forces stabilize the lamellar phase, whereas at high concentrations attractive van der Waals forces are supposed to determine the structure of the L_α phase. One of the first pieces of experimental evidence for undulation forces was given by Safinya *et al.* [30]. They found for a quaternary microemulsion that these forces dominate the interactions between two non-charged lamellae in a range from $4\,\text{nm} < d < 17\,\text{nm}$. In order to understand the stabilizing mechanism in our systems, we calculated the interlamellar distances with the simple geometric model

$$d = 2\frac{v_c}{a_c}\frac{1}{\phi_c} \approx 2\frac{v_c}{a_c}\frac{1}{\gamma} \qquad (6)$$

where v_c is the volume, a_c the area per surfactant molecule, ϕ_c is the volume fraction of the surfactant in the water – surfactant mixture and γ the corresponding mass fraction. With $v_c(C_{10}E_4) = 0.58\,\text{nm}^3$ and $a_c(C_{10}E_4) = 0.53\,\text{nm}^2$ [28] the results shown in figure 8 were obtained. On the basis of neutron reflectivity measurements [31], we estimated the thickness of a hydrated $C_{10}E_4$ bilayer to be $5.0 \pm 0.5\,\text{nm}$. As can be seen in figure 8, the bilayer thickness ε is similar to the interlamellar distance d in a concentration range $0.35 < \gamma < 0.50$. Thus, it is in this range where the crossover from van der Waals to undulation forces takes place. Assuming that the bilayer thicknesses of the described non-ionic surfactants are similar, it is not surprising that the disconnections in figures 2 (*b*) and 7 are observed at similar surfactant concentrations. In other words, the transition from the connected to the disconnected lamellar phase is expected to be at between 35 and 50 wt % surfactant for bilayer thicknesses around 5 nm. We would like to propose that the transition can be tuned by the rigidity of the monolayer. It is in this region where the bilayers are not only very close but also they undulate. Whether or not these undulations lead to the formation of an isotropic phase, and thus to a disconnection of the lamellar region, depends on the rigidity of the monolayer. The higher the rigidity of the monolayer, the greater its ability to resist undulations. Thus, from the results presented here it can be concluded that the disconnection takes place in a concentration range where $\delta \approx \varepsilon$ and that it is tuneable by the rigidity of the monolayer.

4.2.3. *Stacked mono- and bi-layers*

Finally, the transition from the lamellar to the adjacent isotropic phase will be discussed for both the dilute and the concentrated lamellar phases. Our starting point is the separated 'dilute' lamellar phase observed for the $C_{10}E_4/C_{10}E_5$ mixture (see figure 2 (*b*)) and the surfactant $(C_1)_3SiC_6E_5M$ (see figure 7), in the vicinity of which two isotropic phases were found. At low concentrations it is the isotropic L_3 phase that is formed. As already mentioned, the forces acting

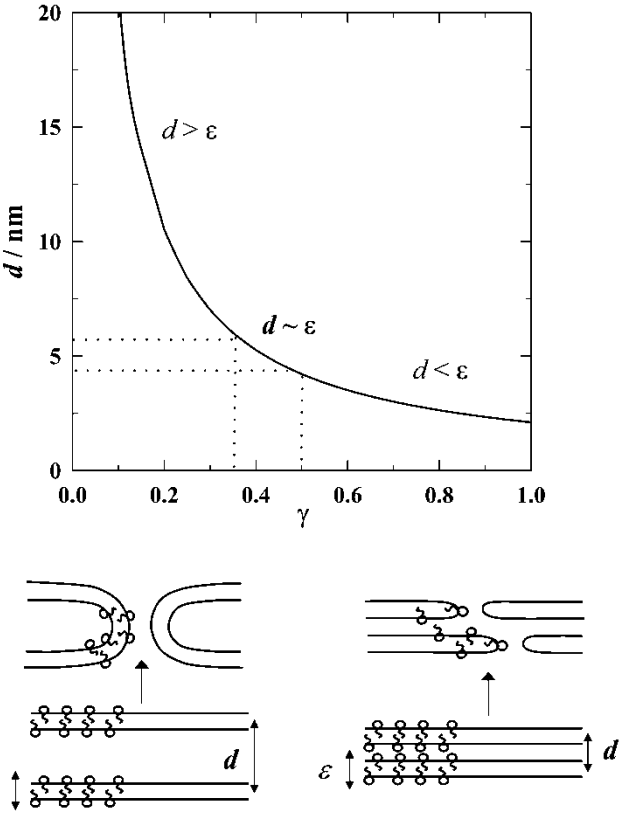

Figure 8. Above: Interlamellar distance d as a function of the surfactant mass fraction γ calculated according to equation (6). The $C_{10}E_4$ bilayer thickness ε was estimated to be $5.0 \pm 0.5\,\text{nm}$ and is indicated by the dotted lines. Below: Schematic drawing of the transient state of passage formation which will lead to a randomly connected bilayer (left) and monolayer (right) network, respectively. The former structure is called the L_3 phase, the latter has not yet been given a name.

between bilayers are at least the attractive van der Waals force and the steric repulsion of the hydrated molecules. For the dilute lamellar phase an additional repulsive undulation force comes into play. Since it is an additional force this might explain that the lamellar phase is stable even at very low surfactant concentrations and high temperatures until thermal fluctuations, i.e. uncoordinated motions of the bilayers, disturb the structure: the L_3 phase forms. The idea is that the undulating bilayers come into contact and form passages, eventually leading to the formation of an isotropic L_3 phase.

The transition from the L_α to the L_3 phase through the intermediate state of passage formation was monitored by freeze fracture electron microscopy (FFEM) [9]. This isotropic phase consists of a bicontinuous network of two aqueous subvolumes separated by a random bilayer network. The transient state of passage formation is shown schematically in figure 8 (below, left side). On the other side of the lamellar 'island', i.e. at high concentrations, an isotropic region abbreviated as 1 is formed. Considering that the distance between the lamellae decreases with increasing surfactant concentration, the process of the L_3 phase formation can be transferred to the process of the formation of the isotropic 1 phase. The only difference is that at high concentrations passages are formed between two monolayers, whereas at low concentrations the passage-forming entitites are bilayers (see figure 8). In other words, it is a question of the repeat distance d, whether the lamellar phase has to be considered as an arrangement of stacked bilayers or stacked monolayers. Based on these arguments we propose that the structure of the isotropic phase formed between the dilute and the concentrated lamellar phase is also bicontinuous. Measurements performed by He *et al.* [32] and Degiorgio *et al.* [33] along an isothermal path through binary phase diagrams support the formation of a bicontinuous structure. He *et al.* [33] investigated a trisiloxane surfactant and found that the structure changes continuously from the L_1 to the L_2 phase via a multi-connected tubular network, which is formed at concentrations between 50 and 70 wt%. Degiorgio *et al.* [33] carried out SANS measurements across the isotropic single phase region of $C_{12}E_8$ from 0 to 100 wt% surfactant and reported a bicontinuous structure at intermediate concentrations. In contrast to bicontinuous microemulsions, where the two subvolumes consist of water and oil, respectively, in the binary systems it is the surfactant itself which takes over the role of the second subvolume. Measurements intended to clarify this point are in progress.

To conclude, the connection or disconnection between the dilute and the concentrated L_α phases depends on the interrelationship of the distance between the monolayers and their rigidity. It may be deduced from the observations made for the different kinds of non-ionic surfactants described, that at surfactant concentrations around 40–50 wt% the distance d between the bilayers is similar to the thickness of the bilayers ε. It is in this concentration range that the monolayers are close enough to form interlamellar attachments. Whether or not these attachments are created depends on the rigidity of the corresponding surfactant layer. We note a striking similarity between the isotropic phase at intermediate concentrations in binary systems and the occurrence of the isotropic symmetric bicontinuous microemulsions in the vicinity of a dilute lamellar phase.

5. Conclusions

We have presented new results on two unusual features concerning lamellar phases (L_α) in binary aqueous solutions of non-ionic surfactants. The first striking feature is the formation of highly dilute L_α phases down to 1 wt% of surfactant, which has been reported for a small number of non-ionic surfactants which are all of the alkyl polyglycol ether type. So far, in this kind of system only 'connected' lamellar phases have been observed, i.e. a phase transition between the dilute and the concentrated L_α phase does not take place. However, for aqueous solutions of one particular trimethylsilane surfactant, two disconnected L_α regions were observed. This second unusual feature raised three questions, each of which we are able to answer.

a. Is the disconnected L_α phase a peculiarity of the silane surfactant or a general feature of non-ionic surfactants? We addressed this question by investigating systematically and precisely the phase behaviour of the binary H_2O – $C_{10}E_4$ system as well as of the pseudo-binary H_2O – $C_{10}E_4/C_{10}E_5$ systems. A mixture of 90 wt% $C_{10}E_4$ and 10 wt% $C_{10}E_5$ was found to form two disconnected lamellar phases. We concluded that the disconnected L_α phase is a general feature of non-ionic surfactants. The disconnection can be tuned simply by mixing two surfactants, one of which forms a continuous L_α phase extending to low concentrations, whereas the other L_α phase is restricted to high concentrations.
b. Are there any structural differences between the connected and the disconnected L_α phases? To monitor the structural evolution we replaced H_2O by D_2O and measured the ^2H NMR spectra of the D_2O – $C_{10}E_4$ and D_2O – $C_{10}E_4/C_{10}E_5$ systems as a function of the surfactant concentration γ. We found a continuous increase of

the quadrupole splitting $\Delta\nu$ with increasing γ, which indicates a continuous structural evolution from a dilute to a concentrated lamellar phase. Furthermore, the splittings were found to be equal for a given surfactant concentration irrespective of the system. Thus, the answer to the second question is that there are no structural differences between the connected and the disconnected L_α phases. In other words, the disconnection does not change the structure of the remaining L_α phases.

c. What is the reason for the disconnection of the L_α phase? In order to answer this question we discussed the stabilizing mechanisms acting in lamellar phases. In the range of concentration and temperature where the distance between two bilayers is higher than the thickness of the bilayer, i.e. $\delta > \varepsilon$, the L_α phase is stabilized by the interplay of the attractive van der Waals force, the steric repulsion of the hydrated headgroups and the repulsive undulation force, whereas for $\delta \leqslant \varepsilon$ the stabilizing force of undulations vanishes. We calculated the distance between the bilayers and found that in the concentration range where the disconnection is observed the bilayer distance and the bilayer thickness are similar, i.e. $\delta \approx \varepsilon$. In this region a crossover from the repulsive undulation force to the sole repulsion being the steric repulsion takes place, i.e. the bilayers come so close that they cannot undulate. It is in this range that in effect the bilayers become monolayers. Whether or not these undulations lead to the formation of an isotropic phase, and thus to a disconnection of the lamellar region, depends on the rigidity of the monolayer. We concluded that the disconnection only takes place if $\delta \approx \varepsilon$ and that it is tuneable by the rigidity of the monolayer.

The authors wish to thank Dr Thomas Sottmann for fruitful interaction and Dr Bernd Schwarz for help with the phase diagram of H_2O – $C_{10}E_4$. We also thank Dipl.-Chem. Christian Frank for the preparation of the NMR samples. The help of Alfred Hasenhindl and Dipl.-Chem. Daniel Burgemeister with the NMR measurements is gratefully acknowledged. C. S. is indebted to the *FCI*, the *DFG* and the *Ministerium für Wissenschaft und Forschung NRW* for financial support.

Appendix 1

As the determination of phase diagrams is very time-consuming we decided on the following procedure to find two disconnected L_α phases. First the T–δ phase diagram of the pseudobinary H_2O – $C_{10}E_4/C_{10}E_5$ system was measured at a constant surfactant concentration of $\gamma = 0.20$ (see figure 9). At this particular γ the H_2O – $C_{10}E_4$ system ($\delta = 0$) forms a dilute lamellar phase between 46 and 55°C, whereas for H_2O – $C_{10}E_5$ ($\delta = 1.0$) only isotropic phases are observed. On adding $C_{10}E_5$ to H_2O – $C_{10}E_4$, i.e. increasing δ, one observes a decrease of the temperature range in which the L_α phase is stable until it vanishes at $\delta = 0.15$. The same effect, namely a destabilization, is seen for the L_3 phase. The tendency to suppress ordered phases is also manifested in the increased range of the isotropic L_1 phase. At $\gamma = 0.20$ the temperature of demixing increases linearly from 26.81 at $\delta = 0$ to 49.46°C at $\delta = 1.0$. To monitor the suppression of the lamellar phase, $\delta = 0.10$ was chosen and the corresponding T–γ phase diagram was determined. At this particular δ the temperature range of the L_α phase was significantly smaller (50–55°C) than that of the binary system (46–55°C) so that a difference between the T–γ phase diagrams for $\delta = 0$ and $\delta = 0.10$ was expected. The result is seen in figure 2. It has to be underlined that the existence of two separate L_α phases cannot be deduced from the T–δ phase diagram shown in figure 9. It is only the tendency to destabilize the L_α phase that is presented.

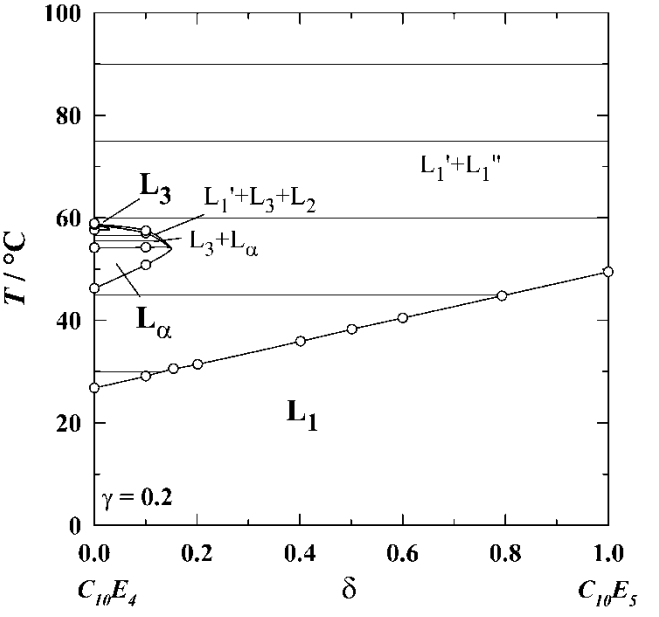

Figure 9. T-δ phase diagram of the pseudobinary H_2O – $C_{10}E_4/C_{10}E_5$ system at $\gamma = 0.20$, where $\delta = 0$ and $\delta = 1.0$ correspond to the binary H_2O – $C_{10}E_4$ and H_2O – $C_{10}E_5$ systems, respectively. It is clearly seen that the range of the lamellar phase decreases with increasing amount of $C_{10}E_5$, i.e. with increasing δ. Note that from this section the existence of two separate lamellar phases cannot be deduced. The notation is the same as in figure 1.

Appendix 2

Figure 10, in comparison with Figure 2(*b*), illustrates the change in phase behaviour upon replacing H_2O by D_2O.

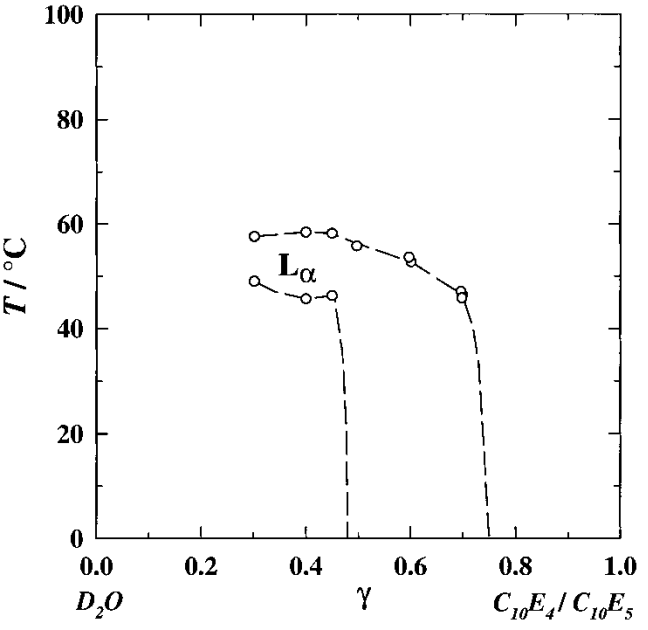

Figure 10. Extension of the lamellar phase in the pseudo-binary D_2O – $C_{10}E_4/C_{10}E_5$ system at $\delta = 0.10$. The phase boundaries (lines) were estimated from the phase transitions (symbols) determined by visual inspection. Comparing figure 10 with figure 2(*b*) one sees that replacing H_2O by D_2O stabilizes the L_α phase at low concentrations, which is reflected in the fact that the

References

[1] KHAN, A., JÖNSSON, B., and WENNERSTRÖM, H., 1985, *J. Phys. Chem.*, **89,** 5180.

[2] FONTELL, K., CEGLIE, A., LINDMAN, B., and NINHAM, B., 1986, *Acta Chem. Scand. A*, **40,** 247.

[3] ZEMB, T., GAZEAU, D., DUBOIS, D., and GULIK-KRZYWICKI, T., 1993, *Europhys. Lett.*, **21,** 759.

[4] STREY, R., SCHOMÄCKER, R., ROUX, D., NALLET, F., and OLSSON, U., 1990, *J. Chem. Soc. Faraday Trans.*, **86,** 2253.

[5] STREY, R., 1996, *Ber. Bunsenges. Phys. Chem.*, **100,** 182.

[6] (*a*) KRATZAT, K. and FINKELMANN, H., 1996, *J. Colloid interface Sci.*, **181,** 542; (*b*) KRATZAT, K., 1999, in *Lyotrope Flüssigkristalle*, edited by H. Stegemeyer (Darmstadt: Steinkopff), pp. 59–106.

[7] (*a*) LI, X., WASHENBERGER, R. M., SCRIVEN, L. E., and DAVIS, H. T., 1999, *Langmuir*, **15,** 2278; (*b*) HILL, R. M., LI, X., and DAVIS, H. T., 1999, in *Silicone Surfactants*, edited by R.M. Hill (New York: Marcel Dekker), pp. 313–348.

[8] WAGNER, R., and STREY, R., 1999, *Langmuir*, **15,** 902.

[9] STREY, R., JAHN, W., PORTE, G., and BASSEREAU, P., 1990, *Langmuir*, **6,** 1635.

[10] MITCHELL, D. J., TIDDY, G. J. T., WARING, L., BOSTOCK, T., and MCDONALD, M. P., 1983, *J. Chem. Soc., Faraday Trans. 1*, **79,** 975.

[11] LANG, J. C., and MORGAN, R. D., 1980, *J. Chem. Phys.*, **73,** 5849.

[12] KRATZAT, K., STUBENRAUCH, C., and FINKELMANN, H., 1995, *Colloid Polym. Sci.*, **273,** 257.

[13] BODEN, N., CORNE, S., and JOLLEY, K., 1987, *J. Phys. Chem.*, **91,** 4092.

[14] GUTMAN, H., LUZ, Z., CHARVOLIN, J., and LOEWENSTEIN, A., 1987, *Liq. Cryst.*, **6,** 739.

[15] GUTMAN, H., LUZ, Z., WACHTEL, E., POUPKO, R., and CHARVOLIN, J., 1990, *Liq. Cryst.*, **7,** 335.

[16] BLACKBURN, J., and KILPATRICK, P., 1992, *Langmuir*, **8,** 1679.

[17] SCHNEPP, W., DISCH, S., and SCHMIDT, C., 1993, *Liq. Cryst.*, **14,** 843.

[18] KRATZAT, K., SCHMIDT, C., and FINKELMANN, H., 1994, *J. Colloid Interface Sci.*, **163,** 190.

[19] STUBENRAUCH, C., FRANK, CH., STREY, R., and SCHMIDT, C., 2002, *Langmuir*, **18,** 5027.

[20] (*a*) SCHUBERT, K.-V., STREY, R., and KAHLWEIT, M., 1991, *J. Colloid Interface Sci.*, **141,** 21; (*b*) SCHUBERT, K.-V., STREY, R., and KAHLWEIT, M., 1991, *Progr. Colloid Polym. Sci.*, **84,** 103.

[21] PAKUSCH, A., 1983, Ph.D. thesis (Göttingen).

[22] DAVIS, J. H., 1983, *Biochim. Biophys. Acta*, **737,** 117.

[23] STREY, R., GLATTER, O., SCHUBERT, K. V., and KALER, E. W., 1996, *J. Chem. Phys.*, **105,** 1175.

[24] KILPATRICK, P. K., BLACKBURN, J. C., and WALTER, T. A., 1992, *Langmuir*, **8,** 2192 and references therein.

[25] ALI, A. A., and MULLEY, B. A., 1978, *J. Pharm. Pharmacol.*, **30,** 205.

[26] LE, T. D., OLSSON, U., MORTENSEN, K., ZIPFEL, J., and RICHTERING, W., 2001, *Langmuir*, **17,** 999.

[27] ORTIZ, A., KILLIAN, J. A., VERKLEIJ, A. J., and WILSCHUT, J., 1999, *Biophys. J.*, **77,** 2003 and references therein.

[28] SOTTMANN, T., STREY, R., and CHEN, H.-S., 1997, *J. Chem. Phys.*, **106,** 6483.

[29] HELFRICH, W., 1978, *Z. Naturforsch.*, **33a,** 305.

[30] SAFINYA, C., ROUX, D., SMITH, G., SINHA, S., DIMON, P., CLARK, N., and BELLOCQ, A., 1986, *Phys. Rev. Lett.*, **57,** 2718.

[31] LU, J. R., LI, Z. X., THOMAS, R. K., BINKS, B. P., CRICHTON, D., FLETCHER, P. D. I., MCNAB, J. R., and PENFOLD, J., 1998, *J. Phys. Chem. B.*, **102,** 5785: by neutron reflection at the water – air interface a monolayer thickness of 2.8 ± 0.4 nm was deduced for $C_{12}E_4$.

[32] (*a*) HE, M., HILL, R. M., LIN, Z., SCRIVEN, L. E., and DAVIS, H. T., 1993, *J. Phys. Chem.*, **97,** 8820; (*b*) HE, M., HILL, R. M., DOUMAUX, H. A., BATES, F. S., DAVIS, H. T., and SCRIVEN, L. E., 1994, in *Structure and Flow in Surfactant Solutions*, edited by C. A. Herb and R. K. Prud'homme (Washington: ACS), pp. 192–216.

[33] DEGIORGIO, V., CORTI, M., and CANTÚ, L., 1988, *Chem. Phys. Lett.*, **151,** 349.